

Impact of Sunlight and Humic Acid on the Deposition Kinetics of Aqueous Fullerene Nanoparticles (nC₆₀)

*Xiaolei Qu, Pedro J.J. Alvarez, and Qilin Li**

Department of Civil and Environmental Engineering, Rice University, Houston TX 77005

* Corresponding author: Qilin Li phone: (713)348-2046; fax: (713)348-5268; email: qilin.li@rice.edu

Environmental Science & Technology

This SI includes a total of 11 pages (including this page) with 4 tables and 6 figures.

QCM-D characterization of particle deposition kinetics

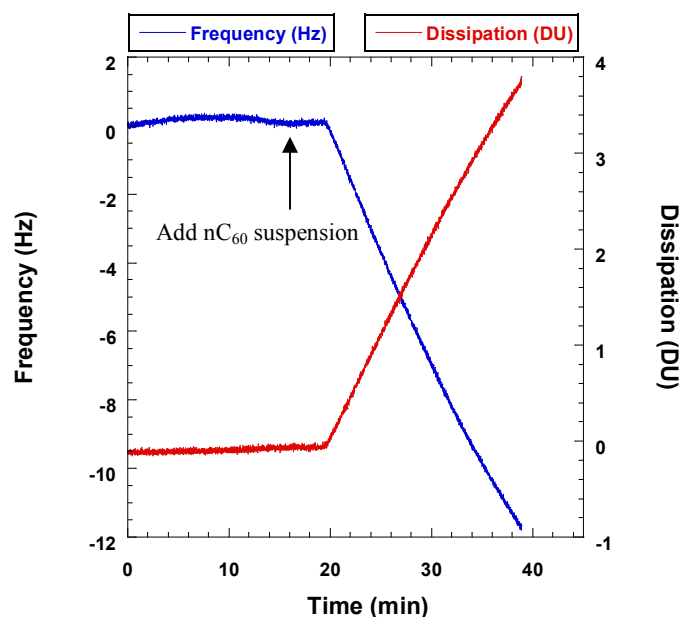


Figure S1. Representative QCM-D measurement data. The figure shows the frequency and dissipation measured at the 3rd overtone as a function of time during the deposition experiment of pristine nC₆₀ onto bare silica surface in 20 mM NaCl solution.

Table S1. The initial slope of the measured 3rd overtone frequency shift Δf_3 and the mass deposition rate calculated by the viscoelastic Voigt model for pristine nC₆₀ deposition on silica surface at various NaCl concentrations.

NaCl (mM)	Δf_3 (Hz/min)	Mass Deposition Rate (ng/cm ² min)
5	0.0615	1.5
10	0.5955	16.7
20	0.6525	19.8
40	0.2385	12
80	0.147	7.2
100	0.099	4.9

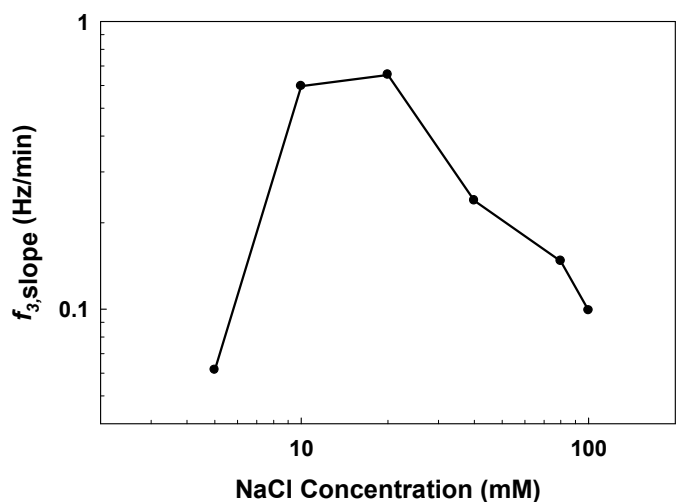


Figure S2a. The initial slop of the measured 3rd overtone frequency shift $f_{3,slope}$ of pristine nC₆₀ deposition on silica surface as a function of NaCl concentration.

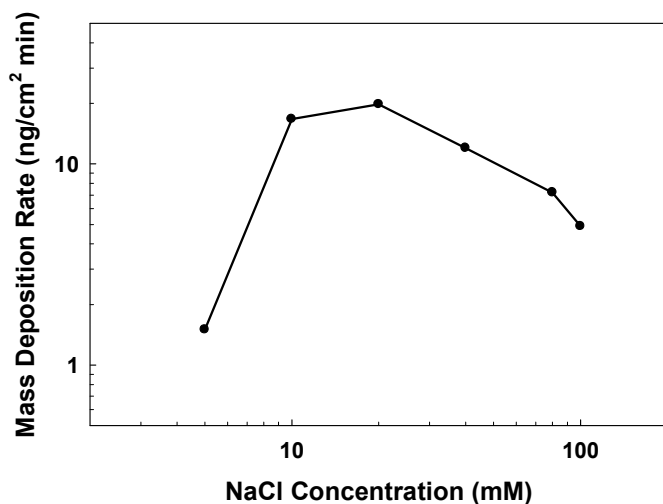


Figure S2b. The mass deposition rate calculated by the viscoelastic Voigt model for pristine nC₆₀ deposition on silica surface as a function of NaCl concentration.

Determination of nC₆₀ particle size in deposition experiments

In the QCM-D experiments, it took 5 min for the nC₆₀ nanoparticles to reach the measurement chamber after being mixed with the NaCl solution. At high ionic strength nC₆₀ aggregation occurred. The nC₆₀ particle size during deposition in the measurement chamber was therefore determined based on the aggregation kinetics curve (average particle size vs. aggregation time) by setting the aggregation time to

39 be 5 min.

40 Table S2. Pristine and 7-day UVA-irradiated (7DUV) nC₆₀ particle size during the QCM-D experiments.

Sample	NaCl concentration (mM)	Particle/aggregate size at 5 min (nm)
Prstine nC ₆₀	1	162
	5	162
	10	162
	20	163.8
	40	241.8
	60	334.5
	80	449.4
	100	492
7DUV nC ₆₀	40	162
	100	162
	150	162
	200	168.9
	250	191.1
	300	244.5
	350	280.8

41

42 **Packed column experiments**

43 Quartz sand sizing from 250 μm to 300 μm in diameter was obtained by sieving a 50 - 70 mesh quartz
44 sand (sigma-aldrich) with 50 and 60 mesh sieves. Before use, the sand was cleaned by soaking in a 1.5
45 M HNO₃ solution for 24 h and rinsing with deionized water until the pH reaches neutral. The sand was
46 then oven dried at 100 °C for 24 h. Columns (Omnifit, 1.5 cm in diameter) were wet packed with clean
47 quartz sand to a height of ~5 cm with a porosity of 0.39 as determined gravimetrically. Figure S3
48 presents the packed column experimental setup. Ten pore volume of deionized water, followed by 10
49 pore volume of background solution, was passed through the column at a flow rate of 2 mL/min to rinse
50 and condition the sand. The nC₆₀ stock suspension and the electrolyte stock solution were mixed to yield
51 the test nC₆₀ suspension at 5 mg/L, which was then introduced into the column at a flow rate of 0.84
52 mL/min until the effluent nC₆₀ concentration reached steady state. The effluent was continuously
53 collected by a fraction collector (Pharmacia Fine Chemicals) and the nC₆₀ concentration was analyzed
54 using a UV-vis spectrophotometer (UV 2550, Shimadazu) at a wavelength of 350 nm. Representative
55 breakthrough curves of nC₆₀ are shown in Figure S4.

56 To create favorable deposition conditions, clean quartz sand was precoated with poly-L-lysine (PLL) by

57 soaking in a solution containing 20 mg/L PLL, 100 mM NaCl and 10 mM HEPES, followed by
58 thoroughly rinsing with deionized water and drying at room temperature.

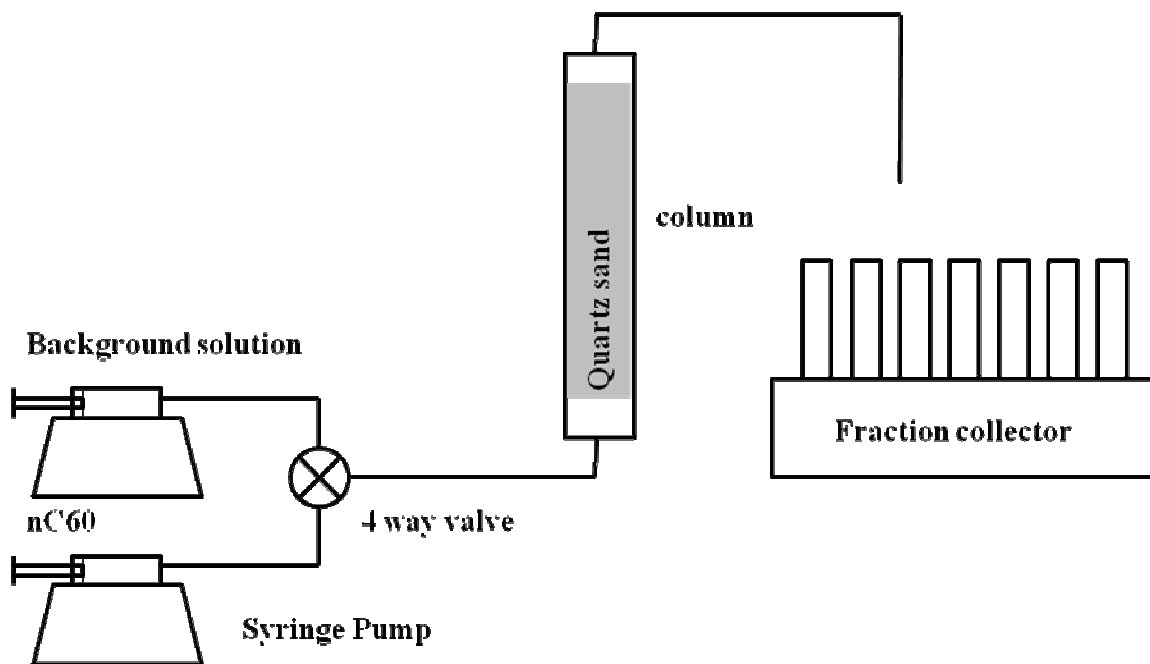
59 The deposition rate coefficient K_d of nC₆₀ in different solution chemistry was determined using
60 following equation: ²

61
$$k_d = -\frac{U}{\varepsilon L} \ln\left(\frac{C}{C_0}\right)$$

62 where U is the superficial velocity, ε is the porosity, L is the column length, C is the steady state effluent
63 concentration of nC₆₀ (i.e., the plateau of the breakthrough curve), and C_0 is the influent nC₆₀
64 concentration.

65 The particle attachment efficiency α was calculated by normalizing the deposition rate coefficient of
66 interest, K_d , by the deposition rate coefficient under favorable conditions, $K_{d,fav}$.

67



68
69 Figure S3. Diagram of the packed column setup

70

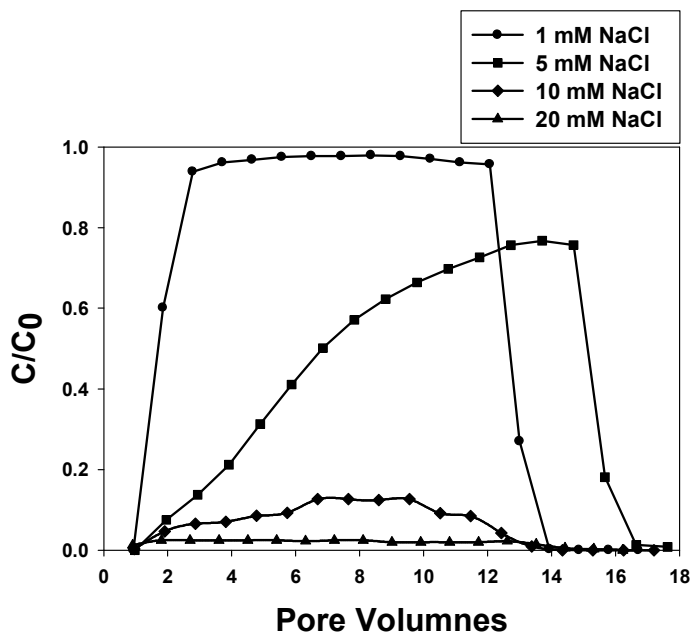


Figure S4. Representative breakthrough curves for nC₆₀ (5 mg/L) transport experiments in silica sand packed columns in NaCl solutions.

The seepage velocity used in the packed column experiments was controlled to match the flow velocity used in the QCM-D experiment. This resulted in similar Peclet number in the two systems.

For the QCM-D system, a parallel-plate channel configuration was assumed:³

$$P_{e\text{ QCM}} = \frac{3v_m a^3}{2b^2 D}$$

Here, v_m is the flow velocity in the measurement chamber, a is the particle radius, b is the half depth of the channel (0.00032 m), and D is the diffusion coefficient. The flow velocity v_m in the QCM-D chamber is 0.0002 m/s at the volumetric flow rate of 100 $\mu\text{L}/\text{min}$. The particle diameter $2a$ at different ionic strength was determined in Table S1. The diffusion coefficient D is estimated using the *Stokes-Einstein* equation:

$$D = \frac{kT}{3\pi\mu d}$$

where k is the Boltzman constant ($1.38 \times 10^{-23} \text{ J} \cdot \text{K}^{-1}$), T is the absolute temperature (298 K), μ is the viscosity of water ($10^{-3} \text{ Pa} \cdot \text{s}$), and the d is the particle diameter.

For packed column system, a sphere in uniform flow configuration was assumed:³

$$P_{\text{column}} = \frac{3A_f v a^3}{R^2 D}$$

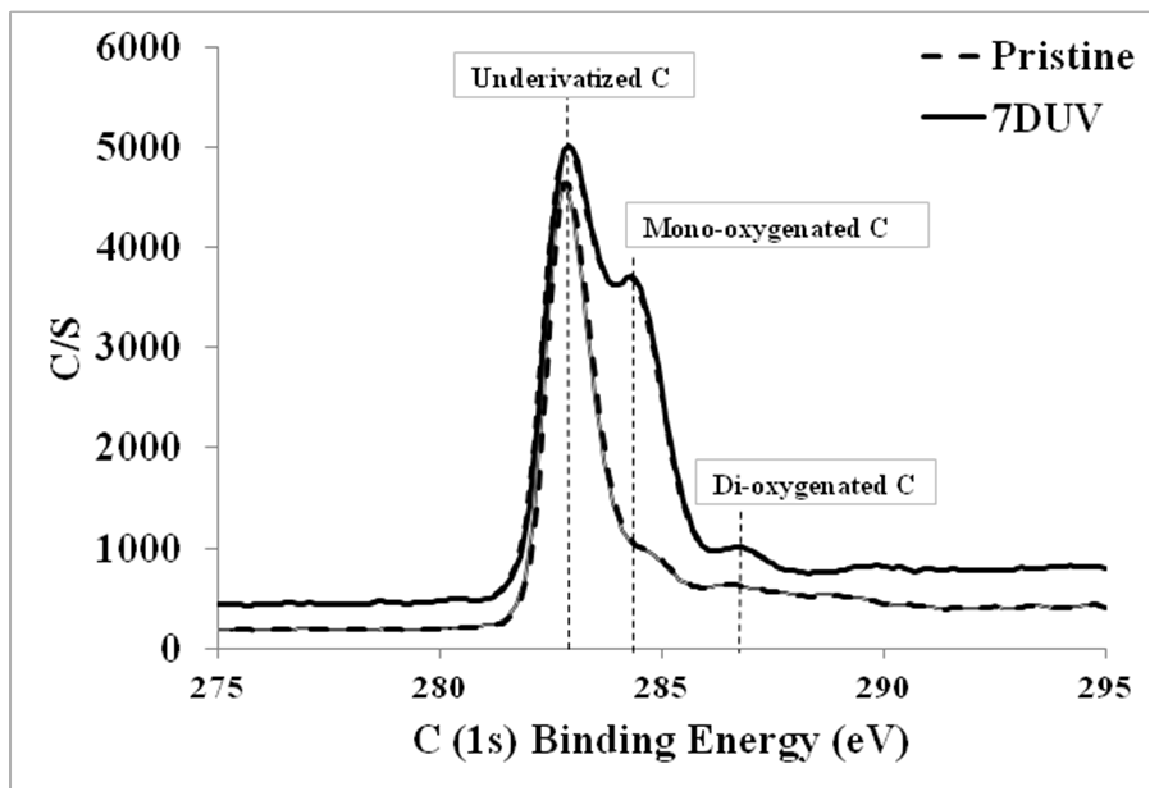
Here, v is the seepage velocity in the column (0.0002 m/s), a is the radius of nC_{60} nanoparticles, R is the radius of silica sands (137.5 μm), and the dimensionless flow parameter A_f is given by:⁴

$$A_f = \frac{3}{2} \left[1 + \frac{0.19 R_e}{1 + 0.25 R_e^{0.56}} \right]$$

Where R_e is the Reynolds number, $R_e = 2vR\rho/\mu$. ρ and μ is the density and viscosity of water respectively.

93

94 **XPS spectra of pristine and 7DUV nC_{60}**



95

96 Figure S5. C(1s) XPS spectra of pristine and 7-day UVA-irradiated (7DUV) nC_{60} .

97

98 **Calculation of DLVO interaction energy between nC_{60} and bare/EHA coated silica surface**

99 The DLVO interaction energy was calculated by assuming sphere-plate interactions. The van der Waals

100 interaction energy was calculated from ²⁴:

101
$$\Phi_v = -\frac{Aa}{6h} \left[1 + \frac{14h}{\lambda} \right]^{-1}$$

102 where A is the Hamaker constant of C₆₀-water-silica system (4.71×10^{-21} J⁷), a is the nanoparticle
103 radius, h is the separation distance, and λ is the characteristic wavelength of the dielectric (normally
104 assumed to be 100 nm).

105 The electrostatic interaction energy was calculated from ²⁵:

106
$$\Phi_E = \pi \varepsilon_0 \varepsilon_r a \left\{ 2\psi_p \psi_c \ln \left[\frac{1 + \exp(-\kappa h)}{1 - \exp(-\kappa h)} \right] + (\psi_p^2 + \psi_c^2) \ln[1 - \exp(-2\kappa h)] \right\}$$

107 where ε_0 is the dielectric permittivity in a vacuum, ε_r is the relative dielectric permittivity of water, a is
108 the nanoparticle radius, κ is the inverse Debye length, h is the separation distance, and ψ_p and ψ_c are the
109 ζ potential of the particle and the silica surface respectively.

110

111 Table S3. Calculated energy barrier between nC₆₀ and bare/EHA coated silica surface at various NaCl
112 concentrations. The ζ potentials used in the calculation are presented in Figure 3b and 6a.

NaCl (mM)	Pristine nC ₆₀ -silica energy barrier (kT)	7DUV nC ₆₀ -silica energy barrier (kT)	Pristine nC ₆₀ -EHA coated silica energy barrier (kT)	7DUV nC ₆₀ -EHA coated silica energy barrier (kT)
5	159.8	-	30.5	-
10	124.4	-	18.5	-
20	93.4	-	13.4	-
40	80.7	139.3	0	0.4
100	42.3	41.4	0	0
150	-	12	-	0
250	-	0	-	0
300	-	0	-	0
350	-	0	-	0

113

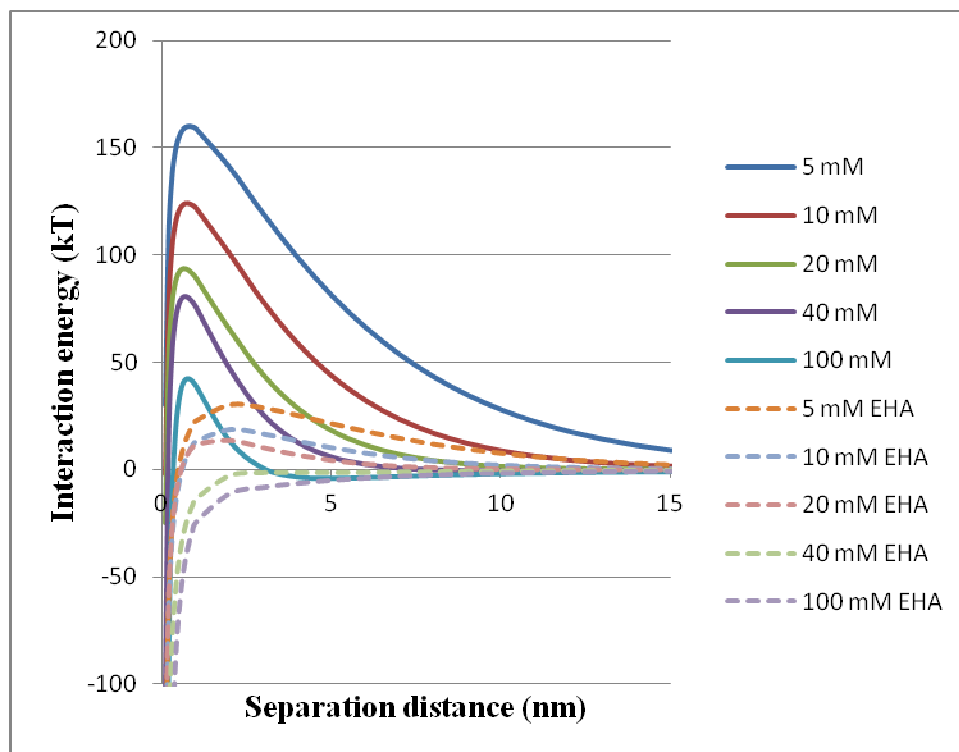


Figure S6a. Calculated DLVO interaction energy profiles for pristine nC_{60} approaching a flat silica or EHA coated silica surface at various NaCl concentrations.

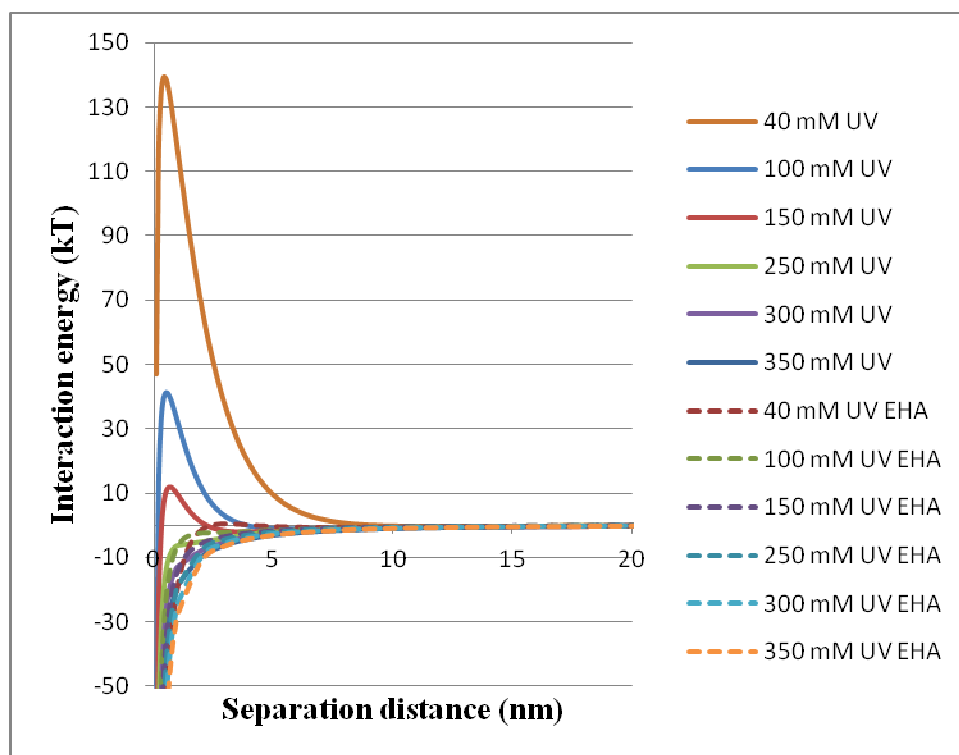


Figure S6b. Calculated DLVO interaction energy profiles for 7-day UVA-irradiated nC_{60} approaching a flat silica or EHA coated silica surface at various NaCl concentrations.

123

124 **Humic acid adsorption experiments**

125 Humic acid (HA) adsorption by the pristine and 7DUV nC₆₀ in deionized water was measured by batch
 126 sorption experiments. The EHA stock solution was filtered through centrifugal filters equipped with 30
 127 kDa MWCO ultrafiltration membranes (Millipor, Carrigtwohill, Co. Cork, Ireland). The resulting EHA
 128 solution was used in the adsorption experiment. Both pristine and 7DUV nC₆₀ solutions were
 129 concentrated using centrifugal filters to 250 mg/L. 1 mg/L EHA was mixed with 200 mg/L nC₆₀ in 10
 130 mL PTFE-lined screw cap glass vials and agitated on a shaker bed at room temperature for 24 h. Then
 131 the samples were filtered with the 30 kDa MWCO centrifugal filters to separate nC₆₀ and the residual
 132 dissolved EHA. The dissolved humic acid concentration was determined by measuring UV absorbance
 133 at 254 nm.

134 Table S4. Humic acid adsorption on pristine nC₆₀ and 7-day UV-irradiated nC₆₀ (7DUV nC₆₀) in 1 mg/L
 135 humic acid solutions. *SRHA adsorption data was reported by our previous paper.¹

	SRHA*	EHA
	K_d (mg/Kg)/(mg/L)	K_d (mg/Kg)/(mg/L)
Pristine nC ₆₀	1722	1648
7DUV nC ₆₀	Non-detectable	Non-detectable

136

137 Adsorption of SRHA onto pristine nC₆₀ nanoparticles in 10 mM and 40 mM NaCl solutions was studied
 138 by QCM-D. After coating the silica crystal surface with PLL, 5 mg/L nC₆₀ in 1 mM NaCl was flowed
 139 across the crystal for 1 h to allow nC₆₀ deposition. The nC₆₀ deposit layer was then rinsed with the
 140 background NaCl solutions. After a stable baseline was achieved, a 5 mg/L SRHA solution in 10 mM or
 141 40 mM NaCl was introduced into the measurement chamber, allowing SRHA to adsorb on nC₆₀ until
 142 reaching adsorption equilibrium. The amount of SRHA adsorbed was calculated using the Sauerbrey
 143 Equation. The SRHA adsorption density on nC₆₀ was quantified by normalizing the total amount of
 144 SRHA adsorbed with the surface area of the crystal.

145

146 **Literature Cited**

147 (1) Qu, X. L.; Hwang, Y. S.; Alvarez, P. J. J.; Bouchard, D.; Li, Q. L., UV Irradiation and Humic
 148 Acid Mediate Aggregation of Aqueous Fullerene (nC(60)) Nanoparticles. *Environ. Sci. Technol.* **2010**,
 149 44, (20), 7821-7826.

- 150 (2) Kretzschmar, R.; Borkovec, M.; Grolimund, D.; Elimelech, M., Mobile subsurface colloids and
151 their role in contaminant transport. *Advances in Agronomy, Vol 66* **1999**, 66, 121-193.
- 152 (3) Gregory, J.; Jia, X.; Williams, R., *Particle deposition and aggregation: measurement, modelling*
153 *and simulation*. Butterworth-Heinemann: 1998.
- 154 (4) Adamczyk, Z.; Warszynski, P.; Szyk-Warszynska, L.; Weronki, P., Role of convection in
155 particle deposition at solid surfaces. *Colloid Surf. A-Physicochem. Eng. Asp.* **2000**, 165, (1-3), 157-187.

156

157